ARTICLE
PUBLISHED ONLINE: 14 NOVEMBER 2016 | DOI: 10.1038/NCHEMBIO.2233

# Tunable thermal bioswitches for *in vivo* control of microbial therapeutics

Dan I Piraner[1–3], Mohamad H Abedi[1–3], Brittany A Moser[1], Audrey Lee-Gosselin[1] & Mikhail G Shapiro[1]*

**Temperature is a unique input signal that could be used by engineered microbial therapeutics to sense and respond to host conditions or spatially targeted external triggers such as focused ultrasound. To enable these possibilities, we present two families of tunable, orthogonal, temperature-dependent transcriptional repressors providing switch-like control of bacterial gene expression at thresholds spanning the biomedically relevant range of 32–46 °C. We integrate these molecular bioswitches into thermal logic circuits and demonstrate their utility in three *in vivo* microbial therapy scenarios, including spatially precise activation using focused ultrasound, modulation of activity in response to a host fever, and self-destruction after fecal elimination to prevent environmental escape. This technology provides a critical capability for coupling endogenous or applied thermal signals to cellular function in basic research, biomedical and industrial applications.**



Rapid advances in synthetic biology[1,2] are driving the development of genetically engineered microbes as therapeutic[3–6] and diagnostic[7–10] agents for a multitude of human diseases. A critical capability for many envisioned applications is the ability to control the function of engineered microbes *in situ* to enable spatially and temporally specific activation at anatomical and disease sites such as the gastrointestinal tract or tumors[2]. However, among existing control methods, systemic chemical administration typically lacks the spatial precision needed to modulate activity at specific anatomical locations, while optical approaches suffer from poor light penetration into tissues[11]. On the other hand, temperature can be controlled both globally and locally—at depth—using technologies such as focused ultrasound[12], infrared light[13] and magnetic particle hyperthermia[14]. In addition, body temperature can serve as an indicator of microbial entry into and exit from the host organism and of the host's condition (e.g., fever).

Notwithstanding this potential, remarkably few high-performance thermal bioswitches are available to control gene expression in engineered microbes. The ideal bioswitch should have a sharp thermal transition resulting in a large change in activity (>100-fold over a few degrees), and its switching temperature should be tunable to enable a broad range of applications. In addition, the bioswitch should be orthogonal to endogenous cellular machinery and compatible with other thermo-responsive components to allow multiplexed thermal logic. Existing temperature-dependent regulators of gene expression—including microbial heat shock factors, membrane-associated proteins, RNA thermometers and transcriptional repressors—fail to fulfill these criteria. Microbial heat shock promoters undergo a relatively low level of thermal induction (~10-fold)[15], have crosstalk with other stimuli such as chemical stress[16] and may be difficult to tune without deleterious effects on the cell. Likewise, the switching temperature of membrane-associated proteins depends on bilayer composition and occupies second-messenger pathways[17]. Meanwhile, RNA thermometers, while orthogonal to the host and amenable to tuning, generally have small dynamic ranges (<10-fold) and broad transitions (>10 °C)[18–23]. Of the available molecular machinery, several natural and mutant transcriptional repressors have the most robust thermal switching and potential for orthogonality[24–30]. However, their relative performance has not been characterized, they have not been systematically engineered to operate at specific transition temperatures, and their potential utility for *in vivo* microbial therapy applications has not been demonstrated.

To address the need for robust, tunable, orthogonal thermal control of engineered microbial systems, we systematically screened candidate transcriptional regulators, developed two orthogonal families of high-performance thermal bioswitches with tunable thresholds within the biomedically relevant range of 32–46 °C, and demonstrated the potential utility of these devices in three distinct *in vivo* scenarios relevant to mammalian microbial therapy. These scenarios include spatially selective activation within a mammalian host using focused ultrasound, sensing and response to a fever, and self-destruction at ambient temperatures to prevent environmental contamination after leaving the intended host.

## RESULTS

### High-performance thermal bioswitches

In order to engineer new families of robust, tunable, orthogonal thermal bioswitches, we began by characterizing the performance of six temperature-dependent transcriptional repressors and six heat shock promoters. Our panel included TlpA, a transcriptional autorepressor from the virulence plasmid of *Salmonella typhimurium*. This protein contains an approximately 300-residue C-terminal coiled-coil domain that undergoes sharp, temperature-dependent uncoiling between 37 °C and 45 °C, and an N-terminal DNA-binding domain that, in its low-temperature dimeric state, blocks transcription from the 52-bp TlpA operator–promoter[24,30]. In addition, we tested a well-known temperature-sensitive variant of the bacteriophage λ repressor cI (mutant $cI^{857}$, here referred to as TcI) acting on a tandem pR–pL operator–promoter[25]. In most previous applications, TcI repression has been modulated via large changes in temperature (e.g., steps from 30 °C to 42 °C)[25]. However, its original description as a virulence factor suggested that much sharper switching may be possible[26]. Alongside TlpA and TcI, we tested four reported temperature-sensitive mutants of the *Escherichia coli* repressors TetR (A89D and I193N)[27] and LacI (A241T and G265D)[28,29], together with a panel of *E. coli* heat shock promoters, including GrpE, HtpG, Lon, RpoH, Clp and DnaK (**Fig. 1a**).

The performance of these constructs is summarized in **Figure 1b**. TlpA and TcI had by far the largest dynamic ranges (355 ± 45 and >1,432, respectively), reflecting a combination of tighter

[1]Division of Chemistry and Chemical Engineering, California Institute of Technology, Pasadena, California, USA. [2]Division of Biology and Biological Engineering, California Institute of Technology, Pasadena, California, USA. [3]These authors contributed equally to this work. *e-mail: mikhail@caltech.edu

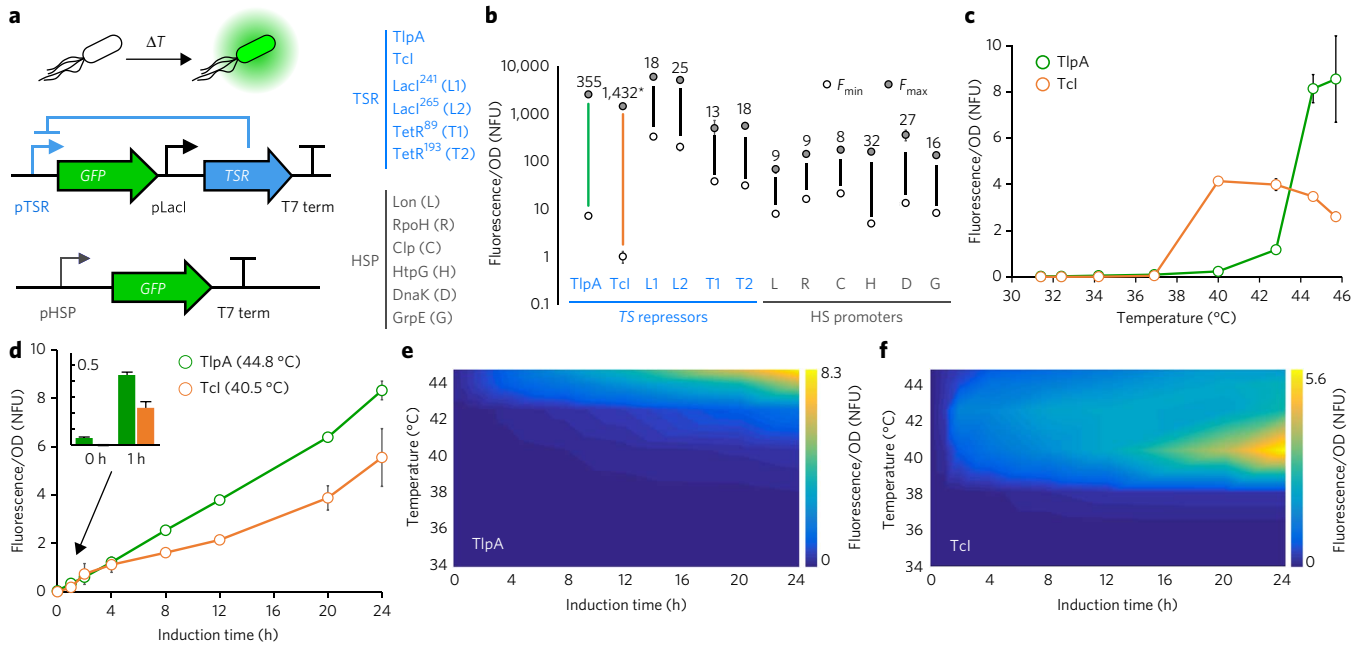


**Figure 1 | High-performance thermal bioswitches.** (**a**) Constructs used to assay the performance of temperature-sensitive repressors (TSR, top) and heat shock promoters (HSP, bottom). The specific repressors and promoters assayed are listed in blue and gray, respectively. (**b**) Optical density (OD)-normalized fluorescence after 12 h of thermal induction for the constructs shown in **a**. NFU, normalized fluorescence units. $F_{min}$ represents expression at 31.4 °C; $F_{max}$ is the maximum fluorescence intensity measured for each construct, measured up to 45.7 °C. The fold changes between $F_{min}$ and $F_{max}$ are listed above each sample. Where not seen, error bars are smaller than the symbol. $N = 4$ for TSRs and $N = 3$ for HSPs. The $F_{min}$ for TcI (indicated by *) is reported from measurement at 34.2 °C because expression at lower temperatures was below the detection limit of the assay. (**c**) OD-normalized fluorescence from the TlpA- and TcI-regulated constructs as a function of induction temperature for a fixed duration of 12 h. $N = 4$. (**d**) OD-normalized fluorescence as a function of thermal induction duration at the maximal induction temperature for the TlpA and TcI constructs. $N = 4$. (**e**,**f**) OD-normalized fluorescence landscapes for TlpA- and TcI-gated constructs, respectively, as a function of both incubation temperature and duration. Data shown interpolated from an 8 × 8 sampling matrix. All samples in **d**–**f** were maintained at 30 °C after the indicated period of thermal induction for a total experimental duration of 24 h before measurement. Error bars represent ± s.e.m.

repression at subthreshold temperatures and stronger promoter activity above threshold. Both of these repressors show sharp thermal transitions, with more than 30-fold induction over ranges of 5 °C and 3 °C centered at 43.5 °C and 39.5 °C for TlpA and TcI, respectively (**Fig. 1c**). Furthermore, both systems are capable of rapid induction, with greater than ten-fold changes in expression observed after a 1-h thermal stimulus (**Fig. 1d**). Complete time-temperature induction profiles for TlpA and TcI are shown in **Figure 1e**,**f**. In addition to their high performance, TlpA and TcI are expected to be more orthogonal to cellular machinery than both the native heat shock promoters and the engineered TetR and LacI repressors, the latter of which are used in multiple endogenous and engineered gene circuits[31–33]. A homology search[34] showed that TlpA and TcI repressors are present in far fewer bacterial species than either TetR or LacI (**Supplementary Results**, **Supplementary Fig. 1**). On the basis of these factors, we chose TlpA and TcI as our starting points for further bioswitch engineering.

Since the behavior of the TlpA operator–promoter has not been studied in *E. coli*, we characterized its molecular mechanisms to inform its utilization in genetic circuits. As shown in **Supplementary Figure 2**, the TlpA operator is a strong promoter (88-fold stronger than $LacI^{Q}$) driven by the transcription factor $\sigma^{70}$. Interestingly, this promoter has bidirectional activity, with identical thermal regulation in both orientations but approximately 200-fold lower maximal expression in the reverse direction (**Supplementary Fig. 2c**,**d**). This property will enable convenient adjustment of TlpA-regulated expression according to circuit requirements.

## Tuning bioswitch activation temperatures

Applications in microbial therapy require thermal bioswitches that activate at different transition temperatures. For example, a host colonization sensor should be activated at 37 °C, whereas a fever detector may work best with a thermal threshold of 39 °C, and a focused ultrasound-activated switch may require a transition point of 41 °C to avoid nonspecific actuation. Synthetic biology applications outside biomedicine may likewise have a variety of thermal requirements. It is thus highly desirable to be able to tune thermal bioswitches to activate at new temperatures while retaining sharp, robust switching performance. To enable such tuning of TlpA and TcI, we devised a simple and effective high-throughput assay based on colony fluorescence. We grew *E. coli* expressing GFP under the control of mutant repressors (generated by error-prone PCR) on solid medium and replica-plated the colonies onto separate plates for simultaneous incubation at desired 'off' and 'on' temperatures (**Supplementary Fig. 3a**). We then imaged the plates through wide-field fluorescence, as shown in **Figure 2a**. As expected, many colonies showed constitutive expression (ostensibly due to loss of repressor function) while others failed to derepress (most likely retaining their original high transition point). However, several colonies showed thermal induction in the desired regime. Within each screen, we selected several such colonies to undergo liquid-phase characterization of induction temperature, switching sharpness and expression levels (**Fig. 2b**). From these variants, we selected mutants that retained the desirable performance characteristics of the wild-type repressor, but with shifted transition temperatures.

Screening of TlpA mutants at off–on temperatures of 30–37 °C and 37–40 °C produced high-performance bioswitches centered at 36 °C and 39 °C, respectively, which we named $TlpA_{36}$ and $TlpA_{39}$ (**Fig. 2c**). For TcI, we selected both downshifted ($TcI_{38}$, $T_m$ = 38 °C) and upshifted ($TcI_{42}$, $T_m$ = 42 °C) variants relative to the original protein (**Fig. 2d**). Together, the engineered TlpA and TcI repressor

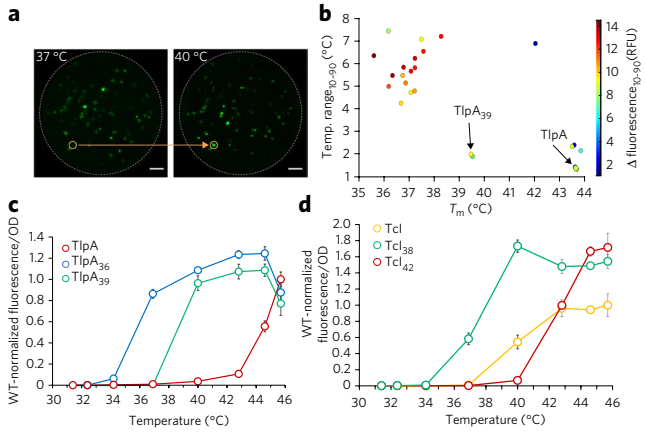


**Figure 2 | Tuning the transition temperature of thermal bioswitches.** (**a**) Fluorescence image of replica plates used to screen for TlpA variants turning on between 37 °C and 40 °C. One colony selected for further assay is indicated by the orange circle. Scale bars, 1 cm. (**b**) TlpA variants plotted by their measured midpoint transition temperatures ($T_{50}$) and 10–90% transition range ($T_{10-90}$), estimated by linear interpolation. The color of each data point maps to the change in fluorescence over the $T_{10-90}$ span. (**c**) OD-normalized fluorescence of the novel TlpA variants normalized to wild type (WT). (**d**) OD-normalized fluorescence of the novel TcI variants normalized to wild type. $N = 4$ for **c** and **d**. RFU, relative fluorescence units. Error bars represent ± s.e.m.

families cover the biomedically relevant range of 32 °C to 46 °C (**Supplementary Fig. 3b**) while demonstrating a dynamic range similar to that of the wild-type protein (**Supplementary Table 1**). The observed decrease in fluorescence at the highest temperatures tested may be due to thermal instability of the cell's transcriptional and translational machinery. The amino acid substitutions identified in these bioswitch variants are shown in **Supplementary Figure 4** and listed in **Supplementary Table 3**. Remarkably, a single round of mutagenesis was sufficient in all cases to obtain at least one variant with the desired switching behavior, suggesting that both TlpA and TcI are highly tunable for a broad range of applications.

## Thermal logic circuits using orthogonal bioswitches

To enable microbial therapy applications, it is useful to develop thermal logic circuits capable of controlling multiple functions at different temperatures or confining activity to within a narrow thermal range. This would enable cells to, for example, initiate one therapeutic function upon host colonization and switch to a different function during a host fever response or local activation with focused ultrasound. We hypothesized that since TlpA and TcI act on orthogonal target sequences, we could combine them in circuits designed for multiplexed thermal control or bandpass activation of microbial function. To assess the first possibility (**Fig. 3a**), we made a construct encoding a GFP modulated by $TlpA_{36}$ and an RFP regulated by TcI (**Fig. 3b**). As predicted, upon exposure to a range of temperatures, the two reporter genes were activated independently at their expected thresholds, with no apparent crosstalk in their induction (**Fig. 3c**). Independent thermal control of the coexpressed circuits is illustrated by spatially patterned bacterial variants incubated at 37 °C and 42 °C (**Fig. 3d**). Next, to develop a thermal bandpass filter (**Fig. 3e**), we engineered a circuit placing the expression of RFP under the control of the lambda promoter, gated by both TcI (turning on above 36 °C) and the temperature-independent wild-type cI repressor, which was itself placed under the control of TlpA (activating above 43 °C) as shown in **Figure 3f**. The cI open reading frame was preceded by a synthetic terminator (BBa_B1002) terminator and a weak ribosome-binding site to reduce buildup of this repressor at 40–43 °C due to leakage of the upstream TlpA operon. This resulted in RFP expression confined between 36 °C and 44 °C, while simultaneously turning on GFP above RFP's turn-off temperature (**Fig. 3g,h**).

## Spatially targeted control using focused ultrasound

After developing TlpA and TcI-based thermal bioswitches, we demonstrated their utility in three prototypical microbial therapy scenarios. First, we tested the ability of thermal bioswitches to mediate spatially selective control of microbial therapies using focused ultrasound, a modality that is well established in its ability to elevate temperatures in deep tissues with millimeter spatial precision[12] and is used clinically to treat diseases such as cancer[35] and essential tremor[36]. Focused ultrasound has been used to activate gene expression in mammalian cells[37], but it has not, to our

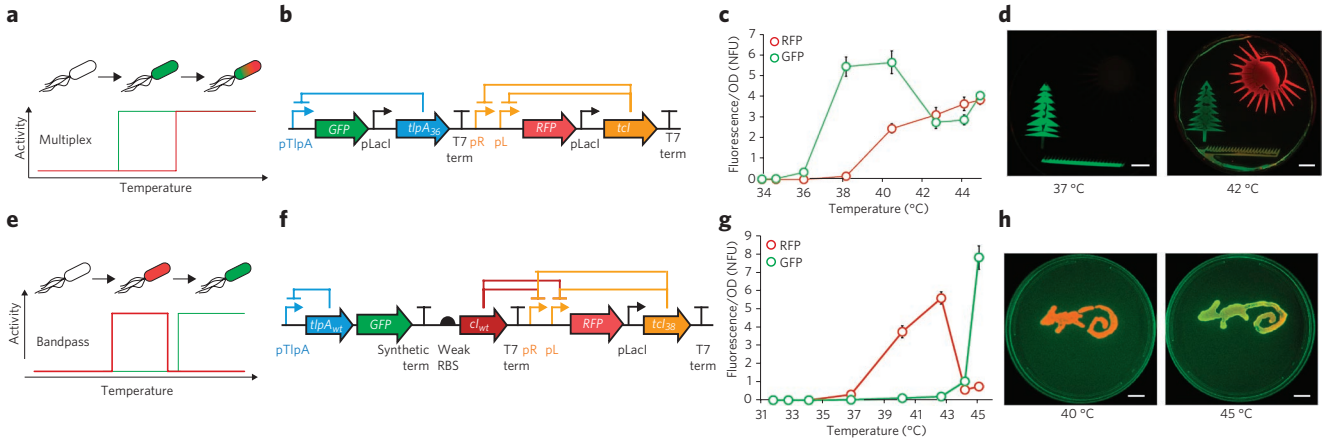


**Figure 3 | Thermal logic circuits.** (**a**) Diagram illustrating multiplexed thermal activation. (**b**) Circuit diagram of the pCali2 plasmid, which contains GFP gated by $TlpA_{36}$ and RFP gated by TcI. (**c**) Expression of GFP and RFP from pCali2-containing *E. coli* over the indicated range of temperatures (12-h incubation). (**d**) Plate images of overlaid GFP and RFP fluorescence from the pCali2 plasmid (grass) and plasmids expressing only the green (tree) and red (sun) components. Note that at 42 °C the grass shows both green and red fluorescence. (**e**) Diagram illustrating a thermal bandpass filter. (**f**) Circuit diagram of the pThermeleon plasmid, in which RFP is gated by $TcI_{38}$ and also by the wild-type cI repressor. GFP is gated by $TlpA_{wt}$ on the same plasmid, which also weakly drives the expression of $cI_{wt}$ through a T7 terminator and weak ribosome-binding site. (**g**) Thermal expression profile of RFP and GFP from pThermeleon-containing *E. coli* (12 h incubation). (**h**) Overlaid GFP and RFP fluorescence images of plated bacteria containing pThermeleon cultured at 40 °C and 45 °C. Scale bars, 1 cm. $N = 4$ for **c** and **g**. Error bars represent ± s.e.m.

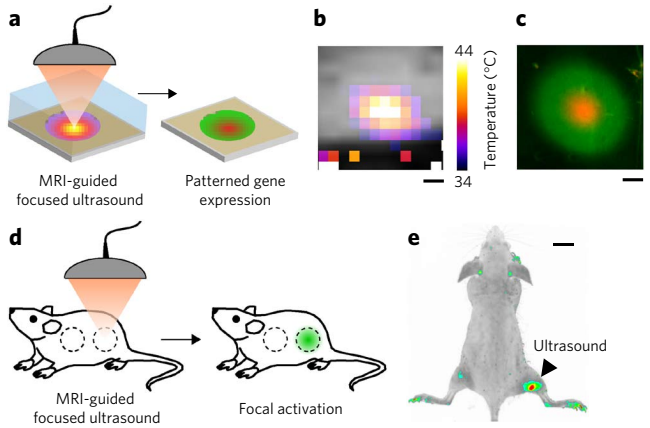


**Figure 4 | Remote control of bacterial agents using focused ultrasound.** (**a**) Illustration of the *in vitro* focused ultrasound experiment: focused ultrasound is used to heat a target area of a bacterial culture lawn through a tofu phantom (depicted as translucent) under MRI guidance, followed by fluorescence imaging. (**b**) MRI-based temperature map of the bacterial specimen during steady-state ultrasound application, overlaid on a raw grayscale MRI image of the phantom. (**c**) Fluorescence image of the region targeted by ultrasound, showing activation consistent with a bacterial construct expressing GFP under the control of $TlpA_{36}$ and RFP regulated by TcI. (**d**) Illustration of the *in vivo* experiment, in which focused ultrasound is used to activate subcutaneously injected bacterial agents at a specific anatomical site. (**e**) Representative thresholded fluorescence map of a mouse injected subcutaneously in both left and right hindlimbs with *E. coli* expressing GFP under the control of $TlpA_{36}$, following ultrasound activation directed at only the right hindlimb. Scale bars, 2 mm (**b**,**c**) and 1 cm (**e**).

knowledge, been employed to control the activity of microbes *in vivo*. Such control could be highly advantageous in applications in which the activity of a systemically administered microbial therapy needs to be localized to a specific anatomical site, such as a deep-seated tumor or section of the gastrointestinal tract, that would be difficult to reach with optogenetic triggers. To test this concept, we first activated gene expression using focused ultrasound in tissue-mimicking phantoms under the guidance of magnetic resonance imaging (MRI)[38] (**Fig. 4a**). This guidance enabled precise spatial targeting of the ultrasound focus and real-time monitoring and adjustment of local temperature. We applied this technique to a flat lawn of *E. coli* containing the multiplexed expression circuit shown in **Figure 3b**. This specimen was assembled with a tissue-mimicking tofu phantom, and steady-state focal heating over 45 min resulted in a radial thermal gradient with an average focal temperature of 42 °C, as observed by real-time MRI thermometry (**Fig. 4b**). A corresponding pattern of spatially localized fluorescence is seen in **Figure 4c**.

To establish the feasibility of this approach *in vivo*, we injected *E. coli* expressing GFP under the control of $TlpA_{36}$ subcutaneously into both hindlimbs of a nude mouse and applied MRI-guided focused ultrasound to one location (**Fig. 4d**) to produce a local steady-state temperature of 41 °C for 45 min to 1 h. This thermal dose is below the damage thresholds for mammalian tissues such as muscle and brain[39,40]. *In vivo* fluorescence imaging 4 h after ultrasound treatment showed robust expression of GFP specifically at the ultrasound-targeted anatomical site (**Fig. 4e**). Two additional animals undergoing the same procedure are shown in **Supplementary Figure 5**. $TlpA_{36}$ was selected as the thermal bioswitch for these experiments because its activation threshold is approximately 4 °C above the typical murine cutaneous temperature[41], a sufficient difference for site-specific ultrasound activation.

### Programmed responses to mammalian host temperature

Next, we sought to develop autonomous thermosensitive microbes responsive to endogenous changes in host temperature. First, we investigated whether bacteria can be engineered to sense and respond to a host fever (**Fig. 5a**). We subcutaneously injected one flank of a nude mouse with *E. coli* expressing GFP under the control of $TlpA_{36}$, and the other flank with *E. coli* expressing GFP controlled by wild-type TlpA as a high-threshold control for nonspecific activation. The mouse was then housed at 41 °C for 2 h in an established fever model paradigm[42]. *In vivo* fluorescence imaging 4 h after fever induction showed robust expression of GFP in the flank injected with $TlpA_{36}$-regulated bacteria (**Fig. 5b**). No significant activation was seen in the opposite flank or in a mouse housed at room temperature (**Fig. 5c**). Two additional replicates of this experiment are shown in **Supplementary Figure 6**.

Second, we tested whether a thermal bioswitch operating at 37 °C could be used to confine the activity of genetically engineered microbes to the *in vivo* environment of a mammalian host and thereby limit the potential for environmental contamination. Toward this end, we designed a genetic circuit in which $TlpA_{36}$ controls the expression of CcdA, a bacterial antitoxin, while constitutively expressing the toxin CcdB, thereby restricting growth to temperatures above 37 °C (**Fig. 5d**). A degradation tag was fused to CcdA to accelerate cell death at nonpermissive temperatures. Bacteria carrying this plasmid grew normally at 37 °C, while bacteria incubated at 25 °C had significantly reduced survival as demonstrated by their colony-forming unit (CFU) counts (**Fig. 5e**). We administered these bacteria to mice by oral gavage and collected fecal pellets after 5 h to allow transit through the gastrointestinal tract. The pellets were kept for 24 h at either 25 °C, corresponding to excretion into the ambient environment, or at 37 °C, equivalent to persistent residence in the gut, and subsequently assayed for colony formation. The survival of cells excreted into ambient temperature was reduced by 10,000-fold as compared to cells maintained under host conditions (**Fig. 5f**).

## DISCUSSION

Our results establish two new families of high-performance, orthogonal thermal bioswitches with tunable activation thresholds to enable a variety of biotechnology applications. Both TlpA- and TcI-based switches respond to temperature with hundreds-fold changes in gene expression. If needed, this response could be further boosted using well-established strategies such as tandem operators and positive feedback amplification[43,44]. In addition, the temporal response of thermal bioswitch circuits could be made either more transient, by manipulating the lifetime of the resulting transcripts and proteins, or longer lasting, by using genetic toggle switches or recombinase-based architectures[28,45]. This may enable persistent functions to be controlled with thermal stimuli shorter than those used in this study.

Our strategy for tuning the thermal response of TlpA and TcI is rapid and simple to implement. The fact that we could identify high-performance variants with new transition temperatures by screening several hundred mutants suggests that many different sequences could satisfy a given thermal requirement. Here, we focused on bioswitches operating between 32 °C and 46 °C, in keeping with potential therapeutic applications and the thermal tolerance of our bacterial chassis. We expect that a similar selection strategy using thermophilic or cryophilic bacteria could be used to tune TlpA and TcI over a yet broader temperature range for industrial applications such as biofuel production. The thermal stability of the regulated gene product will need to be taken into account in these scenarios. Within the temperature range tested in this study, GFP, RFP and CcdA were functional.

The presented bioswitches have sequences orthogonal to bacterial host machinery and to each other, enabling multiplexed thermal

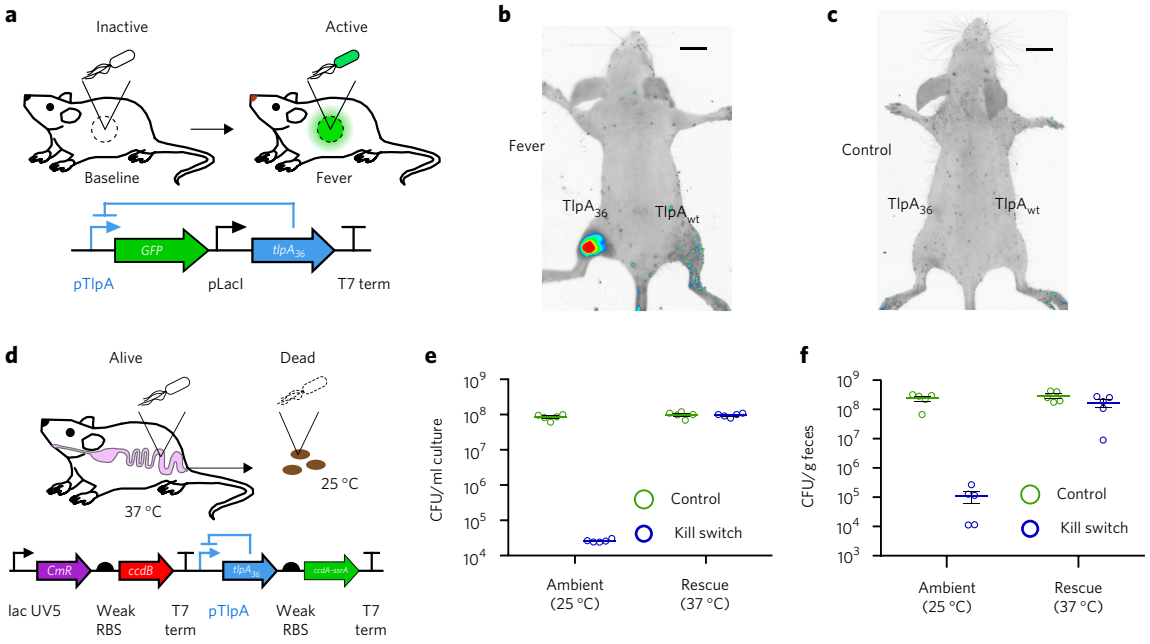


**Figure 5 | Programmed responses to mammalian host temperature.** (**a**) Illustration of the fever-induced activation experiment and circuit diagram of the corresponding *E. coli* construct. (**b**) Representative thresholded fluorescence map of a mouse that underwent fever induction after being injected subcutaneously with plasmids expressing $TlpA_{36}$- and TlpA-regulated GFP into the left and right hindlimbs, respectively. (**c**) Representative thresholded fluorescence map of a mouse that was prepared identically to the animal in **b** but maintained at room temperature. (**d**) Illustration of the temperature-based host confinement strategy, and circuit diagram of the thermal kill switch permitting bacterial survival only at temperatures above 36 °C, at which antitoxin expression is derepressed by $TlpA_{36}$. (**e**) Colony counts from liquid cultures of kill-switch-containing cells and controls (containing no toxin system) after 24 h of incubation at the indicated temperature. $P = 0.0002$ for kill switch versus control cells at 25 °C and $P < 0.0001$ for kill switch at 25 °C versus 37 °C. $N = 5$. (**f**) Colony counts in fecal samples freshly collected from $N = 5$ mice 5 h after oral gavage of kill-switch-containing *E. coli* or controls. The feces were incubated at a temperature representative of post-defecation conditions (25 °C) or were rescued at 37 °C. $P = 0.0067$ for kill switch versus control cells at 25 °C and $P = 0.0275$ for kill switch at 25 °C versus 37 °C. $N = 5$. Error bars represent ± s.e.m. Scale bars, 1 cm.

actuation. If desired, additional multiplexing could be accomplished by replacing the DNA-binding domains of TlpA or TcI with those of other dimeric repressors. Additional engineering may be needed to adapt this technology to other host organisms. Certain species of therapeutic microbes, such as *Lactobacillus* spp., are able to use some promoters transferred directly from *E. coli*[46]. Others may require incorporation of the relevant operator sequences into promoters native to the host[47]. Alternatively, fusions of TlpA and TcI with DNA-binding domains from other microbes or eukaryotes could adapt TlpA and TcI for use in these species.

The three *in vivo* scenarios demonstrated in this work will inform the use of thermal bioswitches in future microbial therapy applications. For example, the ability to detect a host's fever provides a potential safety mechanism with which to curtail effector activity in response to runaway inflammation, a major and sometimes lethal side-effect of antitumor cell therapy[48]. In addition, temperature-dependent kill switches can be used to restrict the survival of enterically administered microbes to host body temperature and thereby mitigate the risk of patients shedding genetically modified, pharmaceutically active organisms into the surrounding environment. Such kill switches can be incorporated into recently developed multilayered and multi-input containment circuits for greater efficiency in preventing mutational escape[49,50]. Furthermore, the ability to activate microbial function at specific anatomical sites using focused ultrasound opens new therapeutic avenues by potentially allowing a physician to locally target therapeutic effects that would be intolerable via systemic administration. Additionally, the ability to trigger gene expression *in vivo* can be combined with genetically encoded genomic or proteomic tools[51–53] to enable the study of cellular signaling within the context of mammalian hosts.

Received 12 May 2016; accepted 16 September 2016; published online 14 November 2016

## METHODS

Methods and any associated references are available in the online version of the paper.

## References

1. Ford, T.J. & Silver, P.A. Synthetic biology expands chemical control of microorganisms. *Curr. Opin. Chem. Biol.* **28**, 20–28 (2015).
2. Fischbach, M.A., Bluestone, J.A. & Lim, W.A. Cell-based therapeutics: the next pillar of medicine. *Sci. Transl. Med.* **5**, 179ps177 (2013).
3. Steidler, L. *et al.* Treatment of murine colitis by *Lactococcus lactis* secreting interleukin-10. *Science* **289**, 1352–1355 (2000).
4. Daniel, C., Roussel, Y., Kleerebezem, M. & Pot, B. Recombinant lactic acid bacteria as mucosal biotherapeutic agents. *Trends Biotechnol.* **29**, 499–508 (2011).
5. Claesen, J. & Fischbach, M.A. Synthetic microbes as drug delivery systems. *ACS Synth. Biol.* **4**, 358–364 (2015).
6. Wells, J.M. & Mercenier, A. Mucosal delivery of therapeutic and prophylactic molecules using lactic acid bacteria. *Nat. Rev. Microbiol.* **6**, 349–362 (2008).
7. Courbet, A., Endy, D., Renard, E., Molina, F. & Bonnet, J. Detection of pathological biomarkers in human clinical samples via amplifying genetic switches and logic gates. *Sci. Transl. Med.* **7**, 289ra283 (2015).
8. Danino, T. *et al.* Programmable probiotics for detection of cancer in urine. *Sci. Transl. Med.* **7**, 289ra28 (2015).
9. Kotula, J.W. *et al.* Programmable bacteria detect and record an environmental signal in the mammalian gut. *Proc. Natl. Acad. Sci. USA* **111**, 4838–4843 (2014).
10. Archer, E.J., Robinson, A.B. & Süel, G.M. Engineered *E. coli* that detect and respond to gut inflammation through nitric oxide sensing. *ACS Synth. Biol.* **1**, 451–457 (2012).
11. Ntziachristos, V. Going deeper than microscopy: the optical imaging frontier in biology. *Nat. Methods* **7**, 603–614 (2010).

12. Haar, G.T. & Coussios, C. High intensity focused ultrasound: physical principles and devices. *Int. J. Hyperthermia* **23**, 89–104 (2007).
13. Huang, X., El-Sayed, I.H., Qian, W. & El-Sayed, M.A. Cancer cell imaging and photothermal therapy in the near-infrared region by using gold nanorods. *J. Am. Chem. Soc.* **128**, 2115–2120 (2006).
14. Thiesen, B. & Jordan, A. Clinical applications of magnetic nanoparticles for hyperthermia. *Int. J. Hyperthermia* **24**, 467–474 (2008).
15. Zhao, K., Liu, M. & Burgess, R.R. The global transcriptional response of *Escherichia coli* to induced sigma 32 protein involves sigma 32 regulon activation followed by inactivation and degradation of sigma 32 in vivo. *J. Biol. Chem.* **280**, 17758–17768 (2005).
16. de Marco, A., Vigh, L., Diamant, S. & Goloubinoff, P. Native folding of aggregation-prone recombinant proteins in *Escherichia coli* by osmolytes, plasmid- or benzyl alcohol-overexpressed molecular chaperones. *Cell Stress Chaperones* **10**, 329–339 (2005).
17. Inda, M.E. *et al.* A lipid-mediated conformational switch modulates the thermosensing activity of DesK. *Proc. Natl. Acad. Sci. USA* **111**, 3579–3584 (2014).
18. Kortmann, J., Sczodrok, S., Rinnenthal, J., Schwalbe, H. & Narberhaus, F. Translation on demand by a simple RNA-based thermosensor. *Nucleic Acids Res.* **39**, 2855–2868 (2011).
19. Neupert, J., Karcher, D. & Bock, R. Design of simple synthetic RNA thermometers for temperature-controlled gene expression in *Escherichia coli*. *Nucleic Acids Res.* **36**, e124 (2008).
20. Waldminghaus, T., Kortmann, J., Gesing, S. & Narberhaus, F. Generation of synthetic RNA-based thermosensors. *Biol. Chem.* **389**, 1319–1326 (2008).
21. Hoynes-O'Connor, A., Hinman, K., Kirchner, L. & Moon, T.S. De novo design of heat-repressible RNA thermosensors in *E. coli*. *Nucleic Acids Res.* **43**, 6166–6179 (2015).
22. Satija, R., Sen, S., Siegal-Gaskins, D. & Murray, R.M. Design of a toolbox of RNA thermometers. Preprint at *bioRxiv* http://dx.doi.org/10.1101/017269 (2015).
23. Wieland, M. & Hartig, J.S. RNA quadruplex-based modulation of gene expression. *Chem. Biol.* **14**, 757–763 (2007).
24. Hurme, R., Berndt, K.D., Namork, E. & Rhen, M. DNA binding exerted by a bacterial gene regulator with an extensive coiled-coil domain. *J. Biol. Chem.* **271**, 12626–12631 (1996).
25. Valdez-Cruz, N.A., Caspeta, L., Pérez, N.O., Ramírez, O.T. & Trujillo-Roldán, M.A. Production of recombinant proteins in *E. coli* by the heat inducible expression system based on the phage lambda pL and/or pR promoters. *Microb. Cell Fact.* **9**, 18 (2010).
26. Sussman, R. & Jacob, F. Sur un systeme de repression thermosensible chez le bacteriophage lambda d'*Escherichia coli*. *C. R. Hebd. Seances Acad. Sci.* **24**, 1517–1519 (1962).
27. Wissmann, A. *et al.* Selection for Tn10 tet repressor binding to tet operator in *Escherichia coli*: isolation of temperature-sensitive mutants and combinatorial mutagenesis in the DNA binding motif. *Genetics* **128**, 225–232 (1991).
28. Chao, Y.P., Chern, J.T., Wen, C.S. & Fu, H. Construction and characterization of thermo-inducible vectors derived from heat-sensitive lacI genes in combination with the T7 A1 promoter. *Biotechnol. Bioeng.* **79**, 1–8 (2002).
29. McCabe, K.M., Lacherndo, E.J., Albino-Flores, I., Sheehan, E. & Hernandez, M. LacI(Ts)-regulated expression as an in situ intracellular biomolecular thermometer. *Appl. Environ. Microbiol.* **77**, 2863–2868 (2011).
30. Hurme, R., Berndt, K.D., Normark, S.J. & Rhen, M. A proteinaceous gene regulatory thermometer in Salmonella. *Cell* **90**, 55–64 (1997).
31. Wilson, C.J., Zhan, H., Swint-Kruse, L. & Matthews, K.S. The lactose repressor system: paradigms for regulation, allosteric behavior and protein folding. *Cell. Mol. Life Sci.* **64**, 3–16 (2007).
32. Bertram, R. & Hillen, W. The application of Tet repressor in prokaryotic gene regulation and expression. *Microb. Biotechnol.* **1**, 2–16 (2008).
33. Jensen, P.R., Westerhoff, H.V. & Michelsen, O. The use of lac-type promoters in control analysis. *Eur. J. Biochem.* **211**, 181–191 (1993).
34. Altschul, S.F. *et al.* Gapped BLAST and PSI-BLAST: a new generation of protein database search programs. *Nucleic Acids Res.* **25**, 3389–3402 (1997).
35. Al-Bataineh, O., Jenne, J. & Huber, P. Clinical and future applications of high intensity focused ultrasound in cancer. *Cancer Treat. Rev.* **38**, 346–353 (2012).
36. Elias, W.J. *et al.* A pilot study of focused ultrasound thalamotomy for essential tremor. *N. Engl. J. Med.* **369**, 640–648 (2013).
37. Deckers, R. *et al.* Image-guided, noninvasive, spatiotemporal control of gene expression. *Proc. Natl. Acad. Sci. USA* **106**, 1175–1180 (2009).
38. Fite, B.Z. *et al.* Magnetic resonance thermometry at 7T for real-time monitoring and correction of ultrasound induced mild hyperthermia. *PLoS One* **7**, e35509 (2012).
39. McDannold, N.J., King, R.L., Jolesz, F.A. & Hynynen, K.H. Usefulness of MR imaging-derived thermometry and dosimetry in determining the threshold for tissue damage induced by thermal surgery in rabbits. *Radiology* **216**, 517–523 (2000).
40. McDannold, N., Vykhodtseva, N., Jolesz, F.A. & Hynynen, K. MRI investigation of the threshold for thermally induced blood-brain barrier disruption and brain tissue damage in the rabbit brain. *Magn. Reson. Med.* **51**, 913–923 (2004).
41. Rudaya, A.Y., Steiner, A.A., Robbins, J.R., Dragic, A.S. & Romanovsky, A.A. Thermoregulatory responses to lipopolysaccharide in the mouse: dependence on the dose and ambient temperature. *Am. J. Physiol. Regul. Integr. Comp. Physiol.* **289**, R1244–R1252 (2005).
42. Pritchard, M.T. *et al.* Protocols for simulating the thermal component of fever: preclinical and clinical experience. *Methods* **32**, 54–62 (2004).
43. Illing, A.C., Shawki, A., Cunningham, C.L. & Mackenzie, B. Substrate profile and metal-ion selectivity of human divalent metal-ion transporter-1. *J. Biol. Chem.* **287**, 30485–30496 (2012).
44. Nistala, G.J., Wu, K., Rao, C.V. & Bhalerao, K.D. A modular positive feedback-based gene amplifier. *J. Biol. Eng.* **4**, 4 (2010).
45. Andersen, J.B. *et al.* New unstable variants of green fluorescent protein for studies of transient gene expression in bacteria. *Appl. Environ. Microbiol.* **64**, 2240–2246 (1998).
46. Natori, Y., Kano, Y. & Imamoto, F. Characterization and promoter selectivity of Lactobacillus acidophilus RNA polymerase. *Biochimie* **70**, 1765–1774 (1988).
47. Mimee, M., Tucker, A.C., Voigt, C.A. & Lu, T.K. Programming a human commensal bacterium, *Bacteroides thetaiotaomicron*, to sense and respond to stimuli in the murine gut microbiota. *Cell Syst.* **1**, 62–71 (2015).
48. Tey, S.-K. Adoptive T-cell therapy: adverse events and safety switches. *Clin. Transl. Immunology* **3**, e17 (2014).
49. Chan, C.T., Lee, J.W., Cameron, D.E., Bashor, C.J. & Collins, J.J. 'Deadman' and 'Passcode' microbial kill switches for bacterial containment. *Nat. Chem. Biol.* **12**, 82–86 (2016).
50. Gallagher, R.R., Patel, J.R., Interiano, A.L., Rovner, A.J. & Isaacs, F.J. Multilayered genetic safeguards limit growth of microorganisms to defined environments. *Nucleic Acids Res.* **43**, 1945–1954 (2015).
51. Lang, K. & Chin, J.W. Cellular incorporation of unnatural amino acids and bioorthogonal labeling of proteins. *Chem. Rev.* **114**, 4764–4806 (2014).
52. Handley, A., Schauer, T., Ladurner, A.G. & Margulies, C.E. Designing cell-type-specific genome-wide experiments. *Mol. Cell* **58**, 621–631 (2015).
53. Grammel, M. & Hang, H.C. Chemical reporters for biological discovery. *Nat. Chem. Biol.* **9**, 475–484 (2013).


## Acknowledgments

The authors thank J. Szablowski for assistance with focused ultrasound, A. Mukherjee, J. Bois and A. Gluhovsky for helpful discussions, and S. Zemsky, R. Rezvani, Y. Jiang and G. Ha for experimental assistance. D.I.P. was supported by the NIH fellowship for Predoctoral Training in Biology and Chemistry (T32GM007616). M.H.A. was supported by an NSF graduate research fellowship and the Paul and Daisy Soros Fellowship for New Americans. This work was supported by a DARPA Young Faculty Award (D14AP00050), the Weston Havens Foundation, a Burroughs Wellcome Career Award at the Scientific Interface and the Heritage Medical Research Institute (M.G.S.).

## Author contributions

D.I.P. co-conceived and planned the study, generated genetic constructs, evaluated their performance *in vitro* and *in vivo*, and co-wrote the manuscript. M.H.A. co-conceived and planned the study, generated genetic constructs, evaluated their performance *in vitro* and *in vivo,* and co-wrote the manuscript. B.A.M. generated genetic constructs and evaluated their performance *in vitro*. A.L.-G. conducted *in vivo* experiments. M.G.S. co-conceived and supervised the study and co-wrote the manuscript. All authors provided input on the final manuscript.

## Competing financial interests

The authors declare no competing financial interests.

## Additional information

Any supplementary information, chemical compound information and source data are available in the online version of the paper. Reprints and permissions information is available online at http://www.nature.com/reprints/index.html. Correspondence and requests for materials should be addressed to M.G.S.

## ONLINE METHODS

**Plasmid construction and molecular biology.** All constructs were made via restriction cloning, KLD mutagenesis, or Gibson Assembly using enzymes from New England BioLabs. All plasmids and their sources of genetic material are described in **Supplementary Table 2**. All constructs were cloned in Mach1 *E. coli* (Thermo Fisher) and the sequence-validated plasmids were assayed in NEB10β *E. coli* (NEB). Fluorescent reporters referred to in the text as GFP and RFP are mWasabi and mCherry, respectively[54,55].

**Thermal regulation assay.** 2 mL cultures of 2× YT medium with 100 μg/mL ampicillin were inoculated with a single colony per culture and grown at 30 °C, 250 rpm for 20 h. After dilution to $OD_{600}$ = 0.1 in LB (Sigma) with 100 μg/mL ampicillin, the cells were propagated at 30 °C, 250 rpm for 1.5 h, after which $OD_{600}$ was measured using a Nanodrop 2000c (Thermo Scientific) in cuvette mode every 10 min. At $OD_{600}$ = 0.25, the cultures were dispensed in 25 μL aliquots into 8 well PCR strips with optically transparent caps (Bio-Rad) using a multichannel pipette and placed into a spatial temperature gradient formed by a Bio-Rad C1000 Touch thermocycler with the lid set to 50 °C. The temperature in each thermocycler well was verified using a TEF-30-T thermocouple (J-KEM Scientific) immersed in 25 μL of pure water within a PCR tube. After the prescribed thermal stimulus, PCR strips were removed, vortexed, and spun down on a tabletop centrifuge and the fluorescence was measured using a Stratagene MX3005p qPCR (Agilent). Immediately after measurement, the cultures were diluted with 75 μL LB/Amp and mixed, after which 90 μL of culture was transferred into 96-well plates (Costar black/clear bottom) for measurement of $OD_{600}$ using a SpectraMax M5 plate reader (Molecular Devices). For studies of gene expression as a function of thermal induction time (**Fig. 1d–f**), samples were returned to incubation at 30 °C after their indicated thermal induction periods such that the total experimental duration was 24 h. Fluorescence measurements were made at the end of this period. Gene expression ($E$) was determined according to equation (1):

$$E = \frac{F_{\text{sample}} - F_{\text{blank}}}{\text{OD}_{\text{sample}} - \text{OD}_{\text{blank}}} - \frac{F_{\text{background}} - F_{\text{blank}}}{\text{OD}_{\text{background}} - \text{OD}_{\text{blank}}} \quad (1)$$

Here, $F$ is the raw fluorescence of the given sample and OD is the OD of the given sample at 600 nm. Raw OD measurements for all experiments are provided in **Supplementary Figure 7**. As expected, bacterial growth is highest in the physiological range of 35 °C to 39 °C. The value of blank fluorescence was determined as the average of all 96 wells in a qPCR plate filled with 25 μL LB. Blank OD was taken as the $y$-intercept of a standard curve of 90 μL nonfluorescent *E. coli* cultures whose $OD_{600}$ values were determined by cuvette measurements in a Nanodrop 2000c spectrophotometer (96 samples total). Background fluorescence was measured from a nonfluorescent construct derived by mutating the chromophore of mWasabi[56] in the pTlpA-Wasabi plasmid (pTlpA-Wasabi-NF). Fluorescence measurements for the thermal expression landscapes of TlpA and TcI were performed using the plate reader due to signal saturation of the qPCR at the 24 h time point (Sample $N$ = 3; Background $N$ = 2 for each time point and temperature). Errors from background measurements were propagated by addition in quadrature. Errors from blank measurements were negligible relative to sample-to-sample variation (relative s.d. <2%) and were omitted from the calculation.

**Colony screening for TlpA tuning.** Error-prone PCR was performed on the repressor gene sequences of pTlpA-Wasabi (Stratagene GeneMorph II kit) and pTcI-Wasabi (NEB Taq Polymerase/0.2 mM $MnCl_2$), and the PCR products were inserted into the parent constructs using Gibson Assembly. The resulting libraries were transformed into NEB10β *E. coli* and plated on LB Agar. Following overnight incubation at 30 °C and the appearance of colonies, a Replica-Plating Tool (VWR 25395-380) was used to replicate each seed plate into two receiver plates. One receiver plate was grown overnight at the desired repressed temperature and the other at the intended activation temperature. Upon the appearance of visible colonies, plates were imaged in a Bio-Rad ChemiDoc MP imager using blue epifluorescence illumination and the 530/28 nm emission filter. Images were examined manually for colonies that appeared dark or invisible on the 'off plate' but showed bright fluorescence on the 'on plate'. Approximately $10^3$ colonies were screened per library. These colonies were picked and subjected to the liquid culture thermal activation assay described above, whereupon their thermal induction profile was compared to that of their parent plasmid. Variants that demonstrated sharp switching and large dynamic range between the desired new transition temperatures were sequenced, re-transformed, and assayed using a higher number of replicates.

***In vitro* toxin–antitoxin assays.** NEB10β cells were transformed with the thermally regulated toxin–antitoxin plasmid and allowed to grow at 37 °C overnight. Because reversion of plasmids carrying toxic genes such as CcdB is known to be a common phenomenon, we used a replica plate screen to isolate colonies that maintained a functional thermal kill switch after transformation. To this end, we replica plated the original transformation into two new plates, one incubated at 25 °C and the other maintained at 37 °C. Colonies that grew at the permissive temperature of 37 °C and not at 25 °C were used in downstream *in vitro* or *in vivo* experiments. For *in vitro* experiments, the selected colonies were grown in 2× YT medium with 100 μg/mL ampicillin at 37 °C with shaking until $OD_{600}$ of 0.6 whereupon they were diluted and plated onto LB agar plates. The plates were incubated overnight at either 25 °C or 37 °C, after which colony forming units (CFU) were counted.

**Focused ultrasound.** MRI-guided focused ultrasound treatment was performed using a 16-channel ultrasound generator, motorized MRI-compatible transducer positioning system and an annular array transducer operating at 1.5 MHz (Image Guided Therapy, Pessac, France). Targeting and real-time imaging was performed using a Bruker Biospec/Avance 7T MRI system with RF excitation delivered by a 7.2 cm diameter volume coil and detection via a 3 cm diameter surface coil. Temperature monitoring was performed using a continuously applied Fast Low Angle Shot sequence with a $T_R$ of 75 ms and $T_E$ of 2.5 ms, matrix size of 32 × 32, and varying FOVs as listed below. Phase images were processed in real time using ThermoGuide software (Image Guided Therapy), and temperature was calculated from the per-pixel phase accumulation due to a decrease in proton precession frequency of 0.01 p.p.m./°C.

For *in vitro* heating, 100 μL of a saturated NEB10β culture expressing the temperature-inducible reporter circuit was plated overnight at 30 °C and incubated for approximately 12 h to form a lawn on a plate containing 0.24% w/v LB (Sigma) and 0.32% w/v Bacto Agar (BD). An approximately 3 cm × 3 cm square of agar was excised from the plate and placed, with the bacterial side facing up, onto a comparably sized pad of 1 cm thick extra firm tofu (O Organics) coated with SCAN ultrasound gel (Parker Laboratories) to exclude air at the interface. A 1 cm high plastic washer made by drilling through the lid of a VWR 35 mm plastic tissue culture dish was placed onto the bacteria, and the assembly was inverted and placed onto the surface coil such that the bacterial lawn, facing down, was supported by the washer. The ultrasound transducer was positioned above the assembly, in contact with the tofu through another thin layer of ultrasound gel. To provide a reference to compensate for global phase drift during the experiment, a second piece of tofu was placed within the field of view but spatially separated by a 1 cm air gap from the object under insonation. A fiber optic thermometer (Neoptix T1) was inserted into the reference tofu, and the difference between the MRI-derived reference temperature and thermometer-reported temperature was accounted for at the site of insonation when calculating the true focal heating.

Ultrasound was applied with the focus aimed at the tofu immediately adjacent to the agar layer with manual control of power level and duty cycle so as to maintain a temperature of 41.5–43 °C for 45 min. Imaging was performed as described above with a matrix size of 5.39 × 5.05 cm and a slice thickness of 2 mm. The plate was subsequently returned to 30 °C for 5 h and imaged using a Bio-Rad ChemiDoc MP imager with blue epi-illumination and a 530/28 nm emission filter (mWasabi) and also green epi-illumination and a 605/50 nm filter (mCherry).

**Animal procedures.** All animal procedures were performed under a protocol approved by the California Institute of Technology Institutional Animal Care and Use Committee (IACUC). 9-week-old BALB/c female mice and 4-week-old NU/J 2019 female mice were purchased from Jackson Laboratory (JAX); 4-week-old SCID/SHC female mice were purchased from Charles River.

For *in vivo* ultrasound actuation, *E. coli* expressing the pTlpA36-Wasabi plasmid were grown to OD 0.6, pelleted, and resuspended to OD 24. A 100 µL bolus was injected subcutaneously into both hindlimbs of a nude mouse (SCID or NU/J2019). Mice were anaesthetized using a 2% isoflurane-air mixture and placed on a dedicated animal bed with the surface coil positioned below the target limb of the mouse. Anesthesia was maintained over the course of the ultrasound procedure using 1–1.5% isoflurane. Respiration rate was maintained at 20–30 breaths per minute, and temperature and respiration rate were continuously monitored using a pressure pad (Biopac Systems) and a fiber optic rectal thermometer (Neoptix). The target limb was thermally activated by elevating the temperature to 41 °C and maintaining the elevated temperature for 45 min to 1 h. Temperature monitoring and adjustment was performed as described above for *in vitro* experiments. Following ultrasound treatment, the mouse was returned to its cage for 4 h, anesthetized, and imaged using a Bio-Rad ChemiDoc MP imager with blue epi-illumination and the 530/28 nm emission filter (mWasabi).

For host fever sensing experiments, SCID mice injected with bacteria as described above were housed in an incubator preset to 41 °C for 2 h and control mice were housed at room temperature. Following treatment, all mice were housed at room temperature for 4 h, anaesthetized, and imaged using a Bio-Rad ChemiDoc MP imager with blue epi-illumination and the 530/28 nm emission filter (mWasabi).

Mouse images are representative of three independent *in vivo* experiments. Fever-induced and control mice were littermates randomly selected for each experimental condition. Investigators were not blinded to group allocation because no subjective evaluations were performed.

For host confinement experiments, BALB/c mice were given drinking water containing 0.5 mg/mL of ampicillin for 24 h, and then starved for food overnight. *E. coli* were grown in 2× YT medium containing ampicillin at 37 °C with shaking until $OD_{600}$ of 0.6. Cultures were pelleted and resuspended at $10^8$ cells/mL in PBS containing 1.5% $NaHCO_3$. 200 µL of the suspension was administered orally using a gavage needle. Food was returned to the mice and the drinking water contained ampicillin throughout the entire experiment. Fresh fecal samples were collected from each mouse 5 h after gavage and incubated at 37 °C or 25 °C for 24 h, then weighed, homogenized in PBS at 0.1 g/mL, diluted and plated onto LB agar plates containing ampicillin. Plates were then incubated overnight at 25 °C and 37 °C. Bacterial colonies were counted as described above for *in vitro* toxin–antitoxin experiments. The sample size was $N = 5$ mice, which was chosen based on preliminary experiments indicating that it would be sufficient to detect significant differences in mean values.

**Electrophoretic mobility shift assay.** Interaction between TlpA, $\sigma^{70}$-RNAp holoenzyme and DNA was demonstrated using a gel shift assay. For this, 50 pmol of fluorescein-labeled double stranded DNA representing the TlpA operator with flanking padding sequences (70 base pairs in total) was incubated with either 50 pmol of TlpA protein or 5 Units (8.5 pmol) $\sigma^{70}$-RNAp holoenzyme (NEB M0551S) individually in 50 µL reaction buffer comprising 40 mM Tris-HCl, 150 mM KCl, 10 mM $MgCl_2$, 0.01% Triton X-100 and 1 mM DTT at a pH of 7.5. As a negative control, the wild-type TlpA operator was replaced with a scrambled version. Following incubation at 37 °C for 30 min, 10 µL of the reaction mixture was supplemented with glycerol to a final concentration of 5% and loaded in a nondenaturing 4% polyacrylamide resolving gel. The gel was run at 65 V for 90 min in buffer comprising 45 mM Tris-borate and 1 mM EDTA at a pH of 8.3. DNA was visualized using Bio-Rad ChemiDoc MP imager using blue epifluorescence illumination and the 530/28 nm emission filter.

**Statistics and replicates.** Data is plotted and reported in the text as the mean ± s.e.m. Sample size is $N = 4$ biological replicates in all *in vitro* experiments unless otherwise stated. This sample size was chosen based on preliminary experiments indicating that it would be sufficient to detect significant differences in mean values. *P* values were calculated using a two-tailed unpaired heteroscedastic *t*-test.


54. Ai, H.W., Olenych, S.G., Wong, P., Davidson, M.W. & Campbell, R.E. Hue-shifted monomeric variants of Clavularia cyan fluorescent protein: identification of the molecular determinants of color and applications in fluorescence imaging. *BMC Biol.* **6**, 13 (2008).
55. Shaner, N.C. *et al.* Improved monomeric red, orange and yellow fluorescent proteins derived from *Discosoma* sp. red fluorescent protein. *Nat. Biotechnol.* **22**, 1567–1572 (2004).
56. Kutrowska, B.W., Narczyk, M., Buszko, A., Bzowska, A. & Clark, P.L. Folding and unfolding of a non-fluorescent mutant of green fluorescent protein. *J. Phys. Condens. Matter* **19**, 285223 (2007).






doi:10.1038/nchembio.2233